Experimental study on the collective theory of flux pinning in a high-field superconductor

R. Meier-Hirmer and H. Küpfer
Kernforschungszentrum Karlsruhe, Institut für Technische Physik and Universität Karlsruhe, Institut für Experimentelle Kernphysik, Postfach 3640, 7500 Karlsruhe, Federal Republic of Germany

H. Scheurer
European Communities, Joint Research Centre, Petten, The Netherlands
(Received 10 July 1984)

Homogenized V_3Si crystals were irradiated with fast neutrons at conditions which result in a proportionality between the induced defect density and the neutron fluence. The critical current density is corrected for differences in the fluence dependence of the upper critical field and of the Ginzburg-Landau parameter. The resulting rise of the volume pinning force is investigated as a function of the density of the weak interacting defects. A second power law which points to a collective interaction is observed at low defect densities and at low fields. With increasing defect density and increasing field, this quadratic dependence vanishes abruptly and an almost linear relation dominates. The exponent of this first power law decreases continuously with further increase of field or defect density. These observations are compared with the collective pinning theory.

I. INTRODUCTION

The nondissipative transport current in the mixed state of a type-II superconductor is a result of the interaction of the flux-line lattice (FLL) with defects of the crystal lattice. The force between flux lines and defects compensates the Lorentz force up to a critical value below which the flux lines are prevented from viscous motion. The summation of the elementary pinning forces to the macroscopic volume pinning force F_p is an unsolved problem. One important advance is the conclusion of Brandt[1] that the interaction is of long range, contrary to assumptions made before. This fact invalidates the common assumption of a single-particle pinning for weakly interacting defects, which implies a linear dependence of the volume pinning force on the concentration of defects; i.e., a dilute concentration does not exist. With this idea as a basis, Larkin and Ovchinnikov,[2] Kerchner,[3] and Matsushita and Yamafuji[4] calculated the volume pinning force for weak pins. Within the framework of the single-particle pinning these weakly interacting defects should cause no pinning at all, because they will not produce an elastic instability in the FLL due to the weak interaction being below the threshold value.[5,6] But in a nondilute system the interaction is a collective phenomenon resulting in a nonzero critical current even for such weakly interacting defects. The calculation of the volume V_c within which the defects do not act independently is the main problem of the collective theory. For weakly interacting, pointlike defects, the authors[2,3] came to the same connection between the volume pinning force, the defect concentration N, and the elementary pinning force f_p, respectively: $F_p \sim (N\langle f_p^2\rangle)^2$. The most striking feature of this correlation is the quadratic dependence of the force per unit volume on the density of defects. The experimental proof of this relation is not as easy as it seems because it requires changing the concentration of defects without changing their properties, such as, for example, size, structure, or composition. In a two-dimensional system Kes and Tsuei[7] observed a collective interaction in thin amorphous films and recently Brandt[8] verified this result by computer simulation. In a three-dimensional system there is only the experimental effort of Kerchner *et al.*[9] demonstrating a quadratic dependence in bulk samples with a low Ginzburg-Landau parameter κ. This is in contrast to quite a few earlier observations on low-κ specimens, pointing to a linear dependence despite interaction forces being much below the threshold force. (See, for instance, the data collected by Campbell and Evetts[10] and by Kramer.[11]) Some of these discrepancies may be due to an underestimation of the elementary pinning forces. A recalculation of the influence of the proximity effect on the core interaction force by Matsushita,[12] as well as the quasiparticle scattering theory very recently published by Thuneberg *et al.*,[13] results in much larger elementary forces, especially in low-κ superconductors. But the discrepancies persist or become even larger, considering the connection between critical current and defect structure in high-κ superconductors which are of interest for high-field applications. In this class of superconductors, the relations between coherence length ξ, flux-line distance a, magnetic penetration depth λ, and the characteristic distances of the defect structure are completely different from those in low-κ materials. For the same defect structure this may result in distinct elementary pinning forces, in different field and temperature dependences of the current, or even in various summation mechanisms of the elementary forces.

In the high-field superconductor V_3Si it was shown by Küpfer and Manuel[14] that the pinning force per unit

volume caused by radiation-induced defects does not obey a linear dependence on the defect density. Especially at higher fields and with increasing concentration the volume pinning force becomes increasingly insensitive to changes of the concentration. A similar behavior is observed for grain boundary pinning in Nb_3Sn where in addition a linear dependence of F_p on the inverse grain diameter, i.e., the concentration, seems to be approximately valid at low fields. For other high-κ superconductors, such as NbTi for instance, the situation is even less transparent than in Nb_3Sn, because there is more than one kind of pinning center involved.

The aim of this paper is to determine the concentration dependence of F_p in a high-κ, high-field material in order to examine the validity of the summation theories and the upper limit of the critical current density. This upper limit does not correspond to the direct summation theory for the majority of common defect structures.

We measured in neutron-irradiated V_3Si samples the critical current density, the reversible displacement, the reversible penetration depth, and the restoring force as a function of defect concentration and magnetic field at different temperatures. In this paper we shall only discuss the correlation between concentration and force per unit volume as a first but impressive and powerful test of summation models. Results and discussion on the other quantities are planned to be published in a forthcoming paper.

II. EXPERIMENTAL

A. Sample preparation

Ingots of stoichiometric V_3Si were prepared from 99.7% pure vanadium and 99.999% pure silicon. The compound was first multiple-arc-melted and then homogenized for three weeks under 0.5-bar argon pressure at a temperature of about 1800 °C. After this treatment the residual resistance ratios of the ingots are between 40 and 80. The precipitates of V and V_5Si_3 observed by metallographic examination after arc melting disappeared completely during homogenization. The grain size is in the range between 10^{-3} and 10^{-2} m. Chemical analysis yields less than 0.005 wt. % oxygen and nitrogen.

The cylindrically shaped samples—prepared by the spark-cutting technique—were etched, polished, and then annealed for 2 h at 1500 °C in an argon atmosphere in order to remove the damaged surface. This layer was observed by the measurement of the radial distribution of the critical current density discussed below. The samples were further characterized by the critical temperature T_c, the upper critical field B_{c2}, and by the specific resistance as a function of temperature. The measurements of T_c, $B_{c2}(T)$, and $j_c(B,T)$ as a function of the distance from the surface of the sample were performed by an inductive method as described by Rollins *et al.*[15]

B. Irradiation procedure

The irradiation was performed in the High Flux Reactor (HFR), of the Commission of the European Communities, at Petten (Netherlands). The HFR is a mixed-spectrum materials test reactor, of the swimming-pool type, with a nominal power of 45 MW. For the irradiation, ten samples were selected which were similar in the relevant superconducting parameters and which show a very low critical current density. Table I gives some data for the various samples after irradiation. The Ginzburg-Landau parameter κ was calculated from the residual resistance ratio and from the slope dB_{c2}/dT at T_c. Specimen 1 is a representative for all samples before irradiation. A more complete presentation of the superconducting parameters including nonstoichiometric V_3Si specimens and specific heat measurements is planned to be published.

The samples were in direct contact with the slowly flowing pool water of the reactor, which has a temperature of 35 °C to 40 °C. The heat generated in the samples by γ absorption can be neglected, so that one can assume that the sample temperature was equal to the pool-water temperature, i.e., 35 °C to 40 °C. All irradiations were per-

TABLE I. Some properties of the investigated specimens. Specific resistance $\rho_{20\,K}$ at a temperature of 20 K, superconducting transition temperature T_c, transition width ΔT_c between 10% and 90% of the normal conducting value, slope of the upper critical field dB_{c2}/dT at T_c, and the Ginzburg-Landau parameter κ as a function of the fast-neutron fluence ϕt.

Sample	ϕt (n/m^2)	$\rho_{20\,K}$ ($\mu\Omega$ m)	T_c (K)	ΔT_c (mK)	$dB_{c2}/dT \mid_{T_c}$ (T/K)	κ
1	0	86	16.78	+ 105—65	1.69	17.1
2	10^{19}	92	16.80	+ 110—74	1.67	17.1
3	2×10^{19}	109	16.85	+ 92—88	1.67	17.3
4	10^{20}	116	16.88	+ 81—116	1.69	17.5
5	2×10^{20}	122	16.73	+ 62—35	1.74	17.6
6	5×10^{20}	143	16.73	+ 107—151	1.68	17.6
7	10^{21}	176	16.89	+ 56—60	1.80	18.3
8	2×10^{21}	270	16.88	+ 41—78	1.85	19.4
9	5×10^{21}	386	16.76	+ 69—54	2.27	21.6
10	10^{22}	569	16.48	+ 57—60	2.34	24.0
11	2×10^{22}	1181	15.55	+ 27—27	2.72	29.6

formed in the pool-side facility of the HFR. This is a position at the outside of the reactor pressure vessel where no reflector elements are present between the core and the samples. In all cases the irradiation rig consisted of a simple aluminum tube, placed vertically at the outside of the pressure vessel, at a defined distance from the wall. The fast-neutron fluence specified below was varied between 10^{19} n/m^2 and 2×10^{22} n/m^2. The duration of the irradiation was kept constant at 46.3 h for all samples with two exceptions discussed in the next section.

The different neutron flux densities were obtained by placing the samples at different vertical locations inside the aluminum tube. Prior to the irradiation, a dosimetry run was performed, using the same irradiation rig. A set of 14 Ni activation detectors was irradiated, at reactor full power, for 1 h. Applying the $^{58}Ni(n,p)^{58}Co$ reaction, the flux density at different heights of the irradiation position was determined (Ref. 16).

The flux measured by the $^{58}Ni(n,p)^{58}Co$ reaction covers only the neutrons captured by the nickel detectors. To correct it to the "equivalent fission neutron flux," it is necessary to apply a correction procedure. The equivalent fission neutron flux is the flux that would be obtained if the same reaction rate were measured in a genuine fission spectrum instead of the unknown spectrum of the irradiation device of question. Of course only neutrons above the threshold are detected, but due to the concept of equivalent fission fluence rate, no direct comparison can be made with, e.g., the fluence >1 MeV for an actual neutron spectrum. To obtain this information, calculations have to be done with the help of the neutron spectrum for the interesting irradiation.

This neutron spectrum can be obtained from multigroup calculations, or with the aid of a less sophisticated adjustment procedure. Correction factors for the commonly used thresholds in the position of the irradiation in question are 0.70 for neutrons with energies >1 MeV (used in this paper), and 1.60 for neutrons with energies >0.1 MeV. Details of the counting procedure and the following data treatment as well as an estimation of the uncertainties of this investigation are given in Ref. 16.

Figure 1 gives a typical neutron spectrum from the pool-side facility of the HFR, at 0.0375 m below center line core level, directly applicable for sample 10. In the comparable figures for the positions where the other samples have been placed, the thermal neutron peak is slightly increased due to the greater distance which the neutrons have to pass through water.

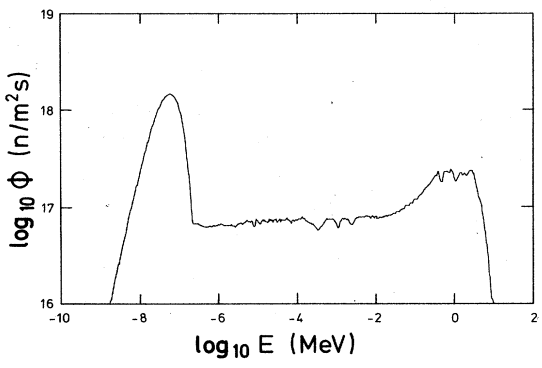

FIG. 1. Neutron spectrum at the irradiation position of the samples in the pool-side facility of the high flux reactor in Petten.

C. Defect concentration and fast neutron fluence

The determination of the defect density and the experimental characterization of the radiation-induced defects is extremely difficult. But only irradiation experiments offer the possibility of varying the concentration of defects by several orders of magnitude, whereas the defect properties remain constant within acceptable limits if the irradiation conditions are suitably chosen. Temperature and flux govern predominantly the kind of defect, the fluence determines its density. At elevated irradiation temperature the primary displacement cascades change their properties first by reformation and collapsing and then they dissolve. The mobile point defects form new secondary defects as dislocation loops or voids. Concentration and size of the stronger interacting voids in V_3Si were determined by transmission electron microscopy by Meier-Hirmer and Küpfer.[17,18] But the aim of this paper is to investigate the more interesting and more common case of weak pins. Therefore we need primary defect cascades or small point-defect clusters, which are the dominant defects at lower irradiation temperature. For these defects the problem of characterization by electron microscopy is not yet solved due to the weak electron-beam contrast of the defects.

At low fluences and at irradiation temperatures below 20 K the density of the primary defect cascades is proportional to the fluence. But this experiment requires that the measurement of the sample is achieved without warming up after irradiation and therefore restricts the sample characterization to one type of measurement, i.e., to one parameter. In order to avoid this disadvantage we decided to irradiate just above room temperature. Under this irradiation condition and without microscopy we run into other difficulties: quantifying the relation between defect density and neutron fluence, and demonstrating that the individual defects remain unchanged at different fluences. The proportionality between density and fluence requires that both irradiation parameters—flux and temperature—have to permit a complete formation of one type of defect during irradiation.

In order to verify this we first collect additional information on the defect structure by discussing the decrease of T_c with increasing fluence in $A15$ compounds. A migration of radiation-induced interstitials or vacancies at higher temperature results in a formation of new defect agglomerations. The diffusion of the point defects decreases the antisite defect concentration, which determines T_c by the degree of disorder. The presence of new defects is therefore correlated with a smaller decrease of T_c as demonstrated in Refs. 17 and 18. Measurements of T_c as a function of fluence made at temperatures between 6 and 420 K by Sweedler *et al.*,[19] Brown *et al.*,[20] and Söll *et al.*[21] on Nb_3Sn, which show the same fluence depen-

TABLE II. Characteristics of three samples irradiated with the same fluence of 10^{21} n/m^{-2}, but for different duration t_{irr}. The last two columns show the estimated differences of the defect concentration, normalized with the concentration N_7 of specimen 7 using the critical current density j_c $[N/N_7(j_c)]$, or the magnetic field B_0 $[N/N_7(B_0)]$, respectively, as discussed in the text.

Sample	t_{irr} (h)	T_c (K)	$\left.\frac{dB_{c2}}{dT}\right\|_{T_c}$ (T/K)	$\frac{N}{N_7}(j_c)$	$\frac{N}{N_7}(B_0)$
12	463	16.78	1.74	0.58	0.70
7	46.3	16.89	1.80	1	1
13	4.63	16.86	1.73	0.82	0.98

dence of T_c as V_3Si and other $A15$ superconductors, reveal no significant dependence on the irradiation temperature. At the irradiation temperature of 310 K we expect therefore collapsed cascades as dominant defects. The properties of the collapsed cascade are governed by the irradiation temperature. At low fluences where the primary defect cascades do not overlap, a linear relation between the density of the collapsed cascades and the fluence is therefore assumed, because no new secondary defects are formed.

As a second point we discuss an experiment made in order to study the influence of time or flux at a constant irradiation temperature. A linear dependence between density and fluence is achieved if the final defect structure does not depend on time or flux but only on fluence, the product of time and flux. This means that the dissolution or alteration of previously formed defects can be neglected. It holds for low fluences and if the irradiation time is long in comparison to the time at the beginning and at the end of the irradiation where constant conditions are not achieved. For that reason we decided to accomplish different fluences by varying the flux as described above. In the preliminary experiment we irradiated three specimens up to the same fluence of 10^{21} n/m^2 at the same temperature of 310 K but with different fluxes. Sample 7 belongs to those samples specified in Table I and was irradiated for 46.3 h, whereas the time for samples 12 and 13 was 463 and 4.63 h, respectively, i.e., the flux was varied by a factor of 100. The properties listed in Table II do not show any differences, although j_c is already affected by the irradiation. Figure 2 shows the critical current density for the three samples as a function of the magnetic field. The measurements are made at temperatures where the upper critical field has the same value of 5.8 T. Neglecting the possible error in the fluence determination, one expects no difference in j_c if the concentration is proportional to the fluence, i.e., independent of flux or time. We choose the fluence of 10^{21} n/m^2 because the critical current density depends very sensitively on the defect density in this fluence region. As shown later in detail the flat part at low fields of the $j_c(B)$ curve obeys $j_c \sim (\phi t)^2$, whereas the field B_0 at which the steep rise in j_c occurs marked with arrows in Fig. 2 decreases approximately linearly with fluence. Using these relations, we can calculate a possible difference in the defect concentration for the investigated specimens. Normalized to the concentration of sample 7, the results obtained are given in Table II.

Comparing samples 7 and 13, one may explain the difference by the uncertainty in the fluence determination. This is plausible because a loss of defects may be expected only with increasing irradiation time, but from samples 7 to 13 the time decreased by a factor of 10. The difference between samples 12 and 7 may be indeed due to dissolved defects during the longer irradiation time in sample 12. The estimated loss of defects in Table II is between 42% and 30%. The flux of sample 12 is equal to that of sample 4, therefore the density of defects increases more than linearly with increasing fluence—about as $N \sim (\phi t)^{1.2}$—in this fluence region up to 10^{21} n/m^2. Because the flux of samples 13 and 10 is equal and if one neglects the small difference between samples 7 and 13 a linear relation between density and fluence above 10^{21} n/m^2 is confirmed.

With this preliminary experiment the dependence of the defect concentration on the fluence was discussed between fluences different by two decades in order to check deviations from the expected linear relation. But the steps in fluence for the investigated specimens are much smaller. By a comparison of samples with neighboring fluences the uncertainties in the proportionality between fluence and defect density are therefore considerably reduced.

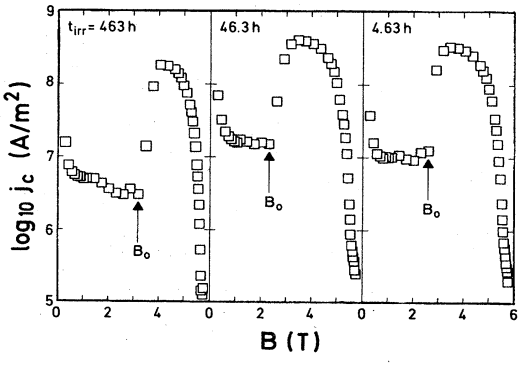

FIG. 2. Critical current density j_c as a function of the field B of three V_3Si samples irradiated at 310 K with the same fast neutron fluence of $\phi t = 10^{21}$ n/m^2 but for different durations t_{irr}. The measuring temperatures are adjusted to values at which the upper critical field corresponds to 5.8 T. At fields B_0, j_c starts to increase.

III. RESULTS

The main purpose is to investigate the concentration dependence of the pinning force density. The starting point of this achievement is the measurement of the critical current density. The inductive method we use allows us to determine the radial profile of the mean local magnetic induction in the cylindrical specimens. As an example Fig. 3 shows the induction versus distance from the surface of sample 11, for different fields. Except for the flat part at the surface and for the following curvature (both are caused by the reversible penetration depth), the derivatives of the field profiles db/dx are independent of the distance.

This corresponds to a homogeneous critical current density. Figure 4 shows this j_c calculated from the magnetic flux profiles as a function of the field at different fluences. From these measurements the pinning force density is obtained by the equation $F_p = Bj_c$.

Because we want to investigate the separate influence of the defect density on the interaction force, we have to eliminate the dependence of F_p on other superconducting parameters. Besides the properties of the defect structure the interaction is determined by B_{c2} and κ:

$$F_p(b,B_{c2},\kappa,\phi t) = CB_{c2}^m(T,\phi t) f(b,\phi t)\kappa^r(\phi t)(\phi t)^{n(b,\phi t)} . \tag{1}$$

C is a constant value and b is the reduced field B/B_{c2}.

First we discuss the influence of the upper critical field. The specimens are all measured at three temperatures at which B_{c2} corresponds to 11.6, 5.8, and 2.9 T, respectively. Figure 5 shows the reduced volume pinning force as a function of the reduced fields measured at the corresponding temperatures for samples 6 and 11. The other samples also obey a temperature scaling behavior $F_p \sim B_{c2}^m(T) \times f(b,\phi t)$ with satisfactory accuracy. The function f describes the field dependence. In Fig. 6 the exponent m is plotted as a function of reduced field at different fluences. The mean value is about 2.5, increasing slightly with increasing field, becoming a maximum at $b \approx 0.95$, and decreasing to 1 at B_{c2}. This is a general behavior observed for all fluences from 10^{19} n/m^2 to 2×10^{22} n/m^2. It demonstrates that the temperature dependence remains the same. In particular, it does not change if the pinning mechanism changes, as discussed later. This uniformity of m and the measurements at the same upper critical fields allows the elimination of the influence of B_{c2} in a comparison of pinning force densities obtained at different fluences, i.e., different concentrations.

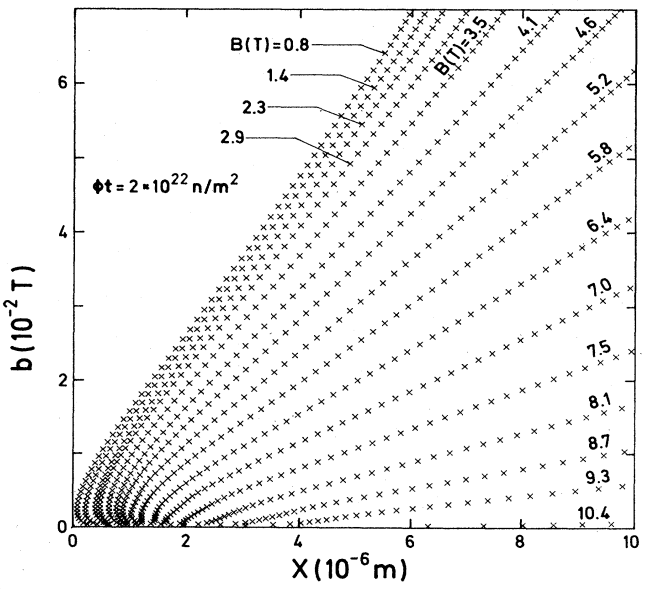

FIG. 3. Radial profile of the local flux distribution b versus distance x for the sample 11. The upper critical field at the measuring temperature is 11.6 T. The x axis starts at the sample surface, the point $b=0$ corresponds to the magnetic field B at which the measurement is made.

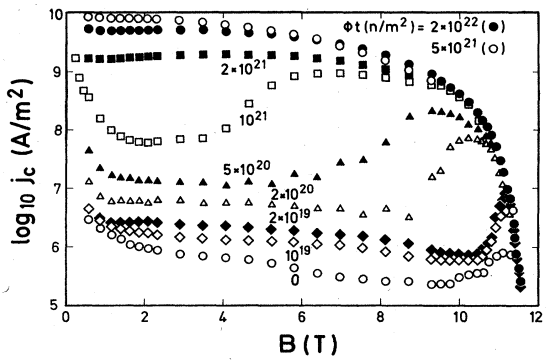

FIG. 4. Critical current density j_c plotted versus magnetic field B for different fast neutron fluences ϕt. All the samples are measured at temperatures at which B_{c2} has the same value of 11.6 T. Certain fluences and some data points in the vicinity of B_{c2} are omitted for clarity.

As a second point we discuss the influence of the Ginzburg-Landau parameter. Table I shows that this quantity increases with decreasing electron mean free path at higher fluences. In this fluence or concentration region we have therefore to account for differences in κ. We can obtain the dependence of F_p on κ in the following way. The influence of the temperature is eliminated by neglecting, in relation (1), the temperature dependence of κ in the investigated temperature region $0.7 \leq T/T_c \leq 0.95$ and by

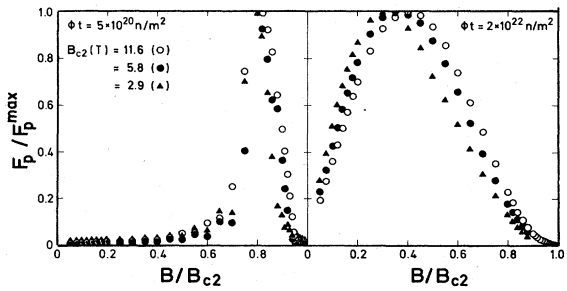

FIG. 5. Normalized volume pinning force F_p/F_p^{max} as a function of the reduced field B/B_{c2} at three different upper critical fields for the samples 6 and 11. Some data points are omitted.

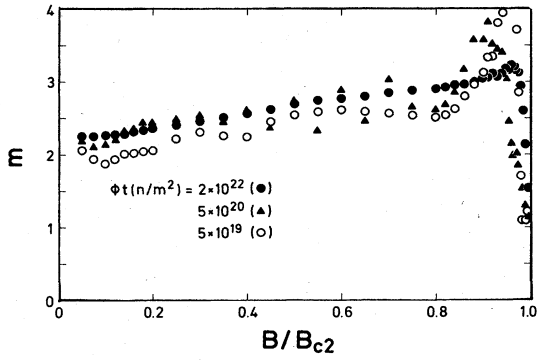

FIG. 6. Mean exponent m of the temperature dependence of the volume pinning force $F_p \sim B_{c2}^m(T)$ versus reduced field B/B_{c2} for three fluences.

comparing only measurements with the same upper critical field. Figure 4 shows that above 2×10^{21} n/m^2 the field dependence of F_p is approximately independent of the fluence. Comparing F_p of three specimens with neighboring fluences we have for each temperature and each field three equations with three unknown quantities f, n, and r from which r can be calculated as a function of B/B_{c2}. Figure 7 shows $r(b)$ in the fluence region between 2×10^{21} n/m^2 and 2×10^{22} n/m^2. From the value presented by the solid line we take $r=-2$ as the exponent for the κ dependence of F_p. The measured F_p values above a fluence of 2×10^{21} n/m^2 were multiplied by the correction factor $[\kappa(\phi t)/17.6]^2$.

As a last step before coming to the defect density dependence of the volume pinning force, we have to account for the background pinning F_{p0} before irradiation. The single-particle theory predicts $F_p=F_{p0}+F_p(\phi t)$, where $F_p(\phi t)$ is the volume pinning force caused by the radiation-induced defects, and F_p is the measured quantity. The collective theory, on the contrary, implies $F_p=\{(F_{p0})^{1/2}+[F_p(\phi t)]^{1/2}\}^2$. At fluences above 5×10^{20} n/m^2, where a correction is not necessary because $F_p \gg F_{p0}$, our results confirm the collective model. This anticipated result enables us to correct for the background pinning within the collective theory. We did this up to the fluence of 10^{21} n/m^2. We used the measured values of the specimens before irradiation which always come close to the representative j_c values of specimen 1 shown in Fig. 4.

The volume pinning force taken from the j_c measurements of Fig. 4, but (as discussed) corrected for the κ variation and for the background current, is shown in Fig. 8. This plot demonstrates the actual rise of the pinning force density due to the radiation-induced defects with increasing fluence. The concentration dependence of the volume pinning force can be divided into three areas. The first one belongs to the fluence region below 2×10^{20} n/m^2. The pinning force density shows a smooth dependence on the magnetic field. There is further an increase in F_p below $B/B_{c2}=0.1$ and a very small but steep rise close to the upper critical field. This last feature becomes dominant in the second region between 2×10^{20} n/m^2 and 10^{21} n/m^2. The peak in F_p broadens at the low-field side and increases violently with increasing fluence. Regarding F_p or j_c in Fig. 4 of the specimen 5, this behavior is well-known as "peak effect." In the field region below B_0 at which the dramatic increase of F_p occurred, F_p behaves similarly to that dominating below a fluence of 2×10^{20} n/m^2 in the whole field region. The third region above 10^{21} n/m^2 is characterized—as the first one—by a smooth F_p-versus-B curve with a maximum at 0.45 reduced field, shifting slightly to lower fields with increasing concentration. At fields above B_p where F_p has a maximum value, F_p increases more slowly with increasing fluence near the upper critical field. This behavior points to a decreasing sensitivity of F_p with increasing defect concentration and increasing field. For still higher fluences it was demonstrated in Ref. 14 and 17 that this saturation becomes even more nearly perfect.

The interaction in the first and third fluence areas in Fig. 8 reveals at a first glance one common feature: The increase of the defect concentration does not influence the

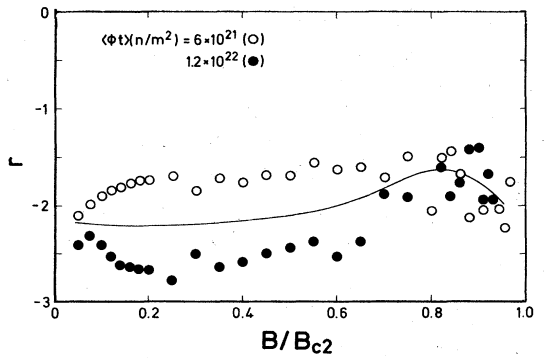

FIG. 7. Mean exponent r of the dependence of the volume pinning force on the Ginzburg-Landau parameter $\kappa(F_p \sim \kappa^r)$ versus reduced field. The given fast neutron fluences denote the mean value of three neighboring fluences used for the calculation. The solid line represents the mean value of both.

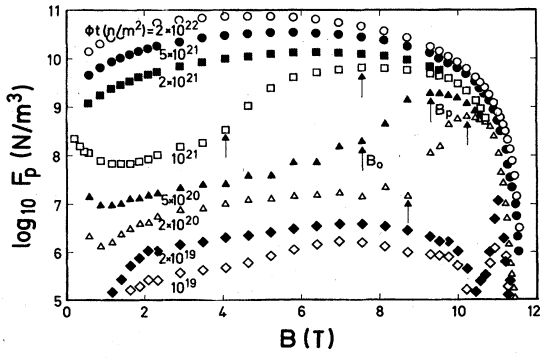

FIG. 8. Increase of the volume pinning force F_p with fast neutron fluences ϕt as a function of the magnetic field B. The values—calculated from the critical current density shown in Fig. 4—are corrected for different Ginzburg-Landau parameters and for the background current as described in the text. The B_0 values are taken from a linear plot of F_p versus B.

field dependence of the pinning force density, i.e., the exponent n in the relation (1) is independent of fluence and field as opposed to the second fluence region. In order to investigate this in more detail we calculate $n(b,\phi t)$ from the quotient of two neighboring fluences. Therefore it is not necessary to consider the discussed deviations from the linear dependence between concentration and fluence. Figure 9 shows n averaged over the measurements taken at different temperatures. We are allowed to do this because F_p obeys a scaling behavior with the same temperature exponent m in the observed field and fluence region. The fluences given in Fig. 9 are the mean values of the two fluences taken for the calculation.

Starting at the lowest fluence of 1.5×10^{19} n/m^2 in Fig. 9(a), we get approximately 2 for the exponent in the field region up to 0.8. At higher fields n increases severely and becomes a maximum. This field region of exceptional influence of the increase of the defect density shifts to lower fields with increasing fluence. The width of this field region broadens because the quotient between two adjacent fluences is kept constant and therefore the actual increase of the concentration is raised with increasing fluence. At fields below this outstanding increase, i.e., below the j_c-peak region, the pinning force density is proportional to

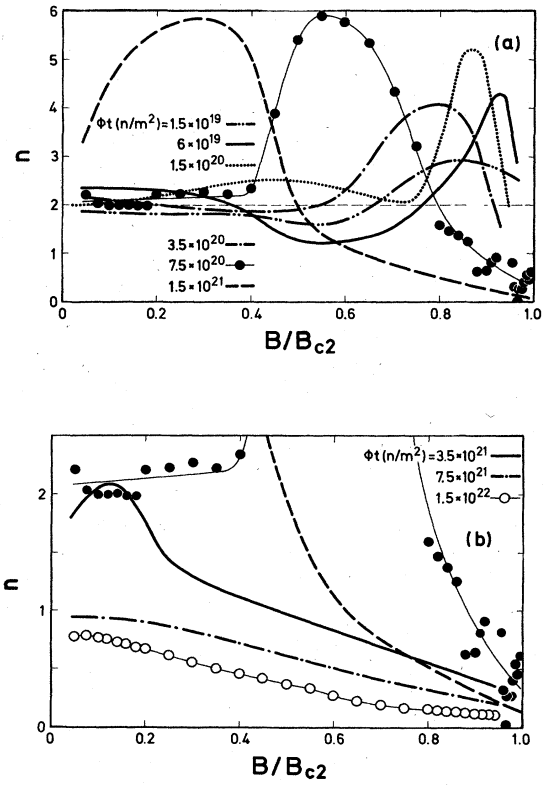

FIG. 9. Exponent n of the concentration dependence of the volume pinning force $F_p\sim(\phi t)^n$ versus reduced field B/B_{c2} up to fluences of 1.5×10^{21} n/m^2 in (a) and from 1.5×10^{21} n/m^2 in (b). The given fluences are the mean values between neighboring fluences used for the calculation. The data points are shown for two fluences only.

the second power of the fluence or of the defect density as proposed by the collective theory. Deviations from the value 2 are within acceptable limits. An error in the determination of the fluence or in the correction for F_{p0} affects the exponent n of the two adjacent values in opposite directions. For instance, in Fig. 9(a), $n(6\times10^{19}$ $n/m^2)$ is below 2 at medium fields, whereas $n(1.5\times10^{20}$ $n/m^2)$ is above 2. The second power law is observed up to a fluence of 7.5×10^{20} n/m^2, where it extends only below $B/B_{c2}=0.4$.

The field region above the exceptional influence of the defect density is characterized by a rapid decrease of n with raised field as well as with raised fluence [Fig. 9(b)]. Above 3.5×10^{21} n/m^2, $n(b)$ is a smooth function decreasing upon approaching the upper critical field. The values of n, for the reduced field, between 0.9 and 1, are spread more than at lower fields due to different transition widths at B_{c2} as shown for the fluence of 7.5×10^{20} n/m^2. This scatter decreases at higher fluences where the transition width becomes smaller.

IV. DISCUSSION

The observed concentration dependence of the pinning force density in the first area, $F_p\sim N^2$ is in accordance with the result of the collective theory of Larkin and Ovchinnikov[2] and Kerchner.[3] We shall discuss certain predictions of the collective model presented by Larkin and Ovchinnikov[2] in comparison with the measurements. In the collective range of pinning the pinning force density is given by the equation

$$F_p=\left[\frac{W}{V_c}\right]^{1/2}=\frac{W^2}{10^8B^2C_{66}^2r_f^3} \tag{2}$$

(in units of N/m^3). V_c is the correlation volume, within which the defects interact collectively with the FLL. For our specimens with weak pinning defects the parameter W is given as $W=N\langle f_p^2\rangle$. The theory claims that this quantity determines the pinning force density throughout the concentration and field regions. The pinning force density of Eq. (2) decreases monotonically with increasing field because the correlation volume is expected to be in the local limit. The volume pinning force of samples 2 and 3 in Fig. 8 has, on the contrary, a maximum at about 0.65 reduced field in the first fluence area. Only at low fields do the measured values show the predicted rise with decreasing field as demonstrated also at lower fields for the sample 7. Ignoring this discrepancy in the field dependence at higher fields we calculate W from the measured F_p by means of Eq. (2). We use the values at about $B/B_{c2}=0.1$ at which F_p has its minimum in the fluence region between 2×10^{20} n/m^2 and 10^{21} n/m^2 where possible errors of the correction for the background current are of minor importance. We use the coherence length as an approximation for the action force radius r_f and take for the shear modulus c_{66} the expression given by Brandt.[22] Considering the field dependence of $f_p\sim\sqrt{b}\,(1-b)$ and the linear relations between W, N, and ϕt we get for $B_{c2}=11.6$ T and $\kappa=17.6$ a mean value

$$W=(1.03\times10^{-21})\phi t b(1-b)^2 \quad (3)$$

(in units of N^2/m^3). The measured temperature dependence of $F_p\sim B_{c2}^{5/2}$, together with Eq. (2), results in a prediction of $W\sim B_{c2}^{7/2}$. Equation (2) should be valid if the condition $R_c k_h \gg 1$ is satisfied. R_c is the transverse size of the correlation volume, and the length $1/k_h$ is a measure of the nonlocality of the elastic behavior of the FLL. With expression (3), the equation $k_h=\sqrt{1-b}\,/\lambda$, and R_c from Eq. (53) in Ref. 2 we calculate the product $R_c k_h$:

$$R_c k_h=\frac{6.73\times10^{23}}{\phi t}b^{3/2}(1-b)^{3/2}(1-0.29b)^{3/2}\ . \quad (4)$$

In the first fluence area the values of $R_c k_h$ are considerably larger than 1. For $R_c k_h \lesssim 1$, Larkin and Ovchinnikov predict a decrease of the correlation volume together with an exponential increase of the pinning force density. Comparing the measurements of F_p in Fig. 8, one finds the product $R_c k_h$ should determine the fields at which F_p starts to increase, i.e., the limit of the first fluence region. This predicted exponential increase of F_p cannot be in accordance with the small rise beyond the minimum of F_p at $b\approx0.1$ but it should rather correspond to the much larger increase at fields marked with B_0 in Fig. 8, where the quadratic dependence of F_p on N vanishes. The smooth rise of F_p between the minimum and B_0 may be due to a continuous transition from local to nonlocal behavior. Using Eq. (4), we can calculate these reduced fields b_0 as a function of fluence if we choose an appropriate constant value for $R_c k_h$ much larger than 1. With $R_c k_h=100$ the relation $B_0/B_{c2}(\phi t)$ shown in Fig. 10 is in agreement with the measured values. Varying the constant does not change the field dependence of Eq. (4), it only shifts the curve above or below the experimental values. Equation (4) explains naturally the striking correlation between field and concentration of defects at which F_p increases rapidly. But the condition (4) has a maximum at $B_0/B_{c2}=0.45$. This means that it is not in accordance with values smaller than 0.45 as observed at $\phi t=10^{21}$ n/m^2 and expected up to 2×10^{21} n/m^2 from Fig. 8. Furthermore, it should be noted from Fig. 8 the increasing uncertainty in B_0 with increasing fluence. But

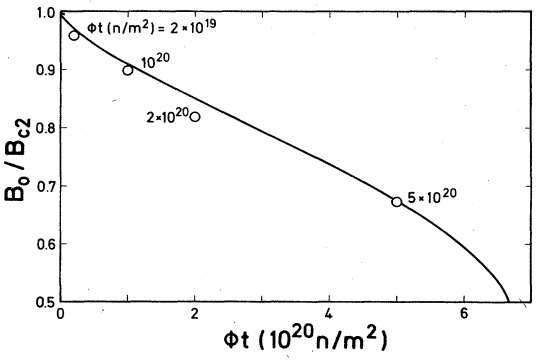

FIG. 10. Reduced fields $b_0=B_0/B_{c2}$ at which the critical current starts to increase as a function of fast-neutron fluence ϕt. The open circles are measured values and the solid line represents Eq. (4) calculated with $R_c k_h=100$ and $\kappa=17.6$.

despite these difficulties, there is another remarkable property of the condition determining B_0. Only using the temperature dependence $W\sim B_{c2}^{7/2}$ deduced above, $R_c k_h$ becomes independent of the temperature in accordance with the observed temperature scaling behavior.

Within the framework of the model the exponential increase of F_p stops if R_c becomes of the order of the flux line distance a, provided that $NV_c \gg 1$, i.e., the number of defects in the correlation volume is large. In the field region where the condition $R_c \approx a$ holds, the pinning force density should obey the relation

$$F_p=\left[\frac{W}{a^2 L_c}\right]^{1/2}\ . \quad (5)$$

L_c is the longitudinal size of the correlation volume in the nonlocal limit given by Eq. (5) or (57) in Ref. 2. With this quantity and W from Eq. (3) we estimated F_p. The experimental values in the high pinning regime are lower by about a factor of 5. This indicates an earlier stop of the decrease of V_c than predicted by $R_c=a$. Kerchner[3] estimated a more precise condition which results in about 3—4 FLL distances.

We use the number of the FLL distances as a parameter q which is determined by means of the measured maximum volume pinning force $F_p^{\max}$ at the corresponding reduced fields b_p:

$$F_p=\left[\frac{W}{q^2a^2L_c^*(qa)}\right]^{1/2}=\frac{1}{q^{5/3}}\left[\frac{W}{a^2L_c}\right]^{1/2}$$
$$\sim N^{2/3}B_{c2}^{5/2}b(1-b)\ . \quad (6)$$

Table III shows the values used for the calculation. The average value results in $q=2.6$, in good agreement with Ref. 3. Using this number, we calculate from Eq. (6) the quantity

$$\frac{F_p^{\max}}{(\phi t)^{2/3}}=(1.12\times10^{-2})b_p(1-b_p) \quad (7)$$

(in units of $N/m^{5/3}$) as a function of the corresponding reduced field b_p as shown in Fig. 11. The measurement agrees within acceptable limits. At fields beyond this maximum—in the third fluence region—F_p should be determined by Eq. (6), which has a maximum at $b=0.5$. This explains the deviation between the experimental points and the theoretical curve at about this field in Fig. 11 because the reduced field of the maximum force should stay constant at 0.5 if $F_p^{\max}/(\phi t)^{2/3}$ results in smaller values. The temperature dependence of Eq. (6) is in satisfying agreement with the experimental result, contrary to the field and concentration dependence. Expression (6) results in a constant exponent of $n=\frac{2}{3}$, whereas the experiment gives a value of n between 2 and 0, continuously decreasing with increasing concentration or field.

A similar transition from N^2 to $N^{2/3}$ is predicted by the flux bundle theory of Kerchner[3] if the elastic behavior of the FLL becomes nonlocal. Furthermore, the equivalence of relation (4) between field and concentration at which the correlation volume shrinks, is about the same

TABLE III. The measured reduced fields $b_0=B_0/B_{c2}$ at which the volume pinning force increases and b_p at which the maximum force $F_p^{max}(b_p)$ is achieved for different fluences ϕt. The values q are the calculated numbers of the flux line lattice distances at which the correlation volume V_c becomes a minimum. The calculation of V_c is made by means of the measured volume pinning force V_c^{expt} and in addition using the corresponding equations of the collective theory V_c^{th} at $B_{c2}=11.6$ T, $\kappa=17.6$, and $B/B_{c2}=0.5$.

ϕt (n/m^2)	b_0	b_p	$F_p^{max}(b_p)$ (N/m^3)	q	V_c^{expt} (m^3)	V_c^{th} (m^3)
1×10^{20}	0.90	0.92	1.86×10^{8}	4.26	1.09×10^{-15}	4.86×10^{-11}
2×10^{20}	0.82	0.88	6.37×10^{8}	3.14	1.16×10^{-16}	6.08×10^{-12}
5×10^{20}	0.68	0.80	1.82×10^{9}	3.09	1.20×10^{-17}	3.89×10^{-13}
1×10^{21}	0.40	0.65	6.40×10^{9}	2.37	7.60×10^{-21}	
2×10^{21}		0.55	1.19×10^{10}	2.27	9.86×10^{-22}	2.73×10^{-21}
5×10^{21}		0.50	3.46×10^{10}	1.73	5.34×10^{-22}	2.01×10^{-21}
1×10^{22}		0.45	5.14×10^{10}	1.80	4.92×10^{-22}	1.59×10^{-21}
2×10^{22}		0.40	7.50×10^{10}	1.85	5.08×10^{-22}	1.26×10^{-21}

in Kerchner's theory if V_c is not constrained by a limited shear strength of the FLL or by two-dimensional defects. A comparison was made by Kerchner[3] between his model and measurements of Küpfer and Manuel[14] on samples prepared similarly to those discussed here. But the steps between neighboring fluences in this former series of specimens, as well as the background current, were too large for the investigation to yield a convincing result.

Figure 12 shows the calculated pinning force densities from Eqs. (2) and (6). The quadratic dependence of F_p on the concentration—as observed in the first fluence region—dominates up to $R_c k_h \gtrsim 100$. The maximum pinning force density is obtained at the corresponding field of the condition $R_c \approx 2.6a$. The predicted exponential increase of F_p between B_0 and B_p was not calculated. From Fig. 12 it becomes obvious that a calculation of n in those field regions where two different mechanisms overlap is meaningless, because it results from a division of F_p values of distinct origins. This is the reason for the maximum of n in Figs. 9(a) and 9(b). The predicted exponential increase of F_p with increasing N cannot be observed by the experiment because the steps between two neighboring fluences are too large.

At fluences above 2×10^{21} n/m^2 this second mechanism, which results in a much larger F_p, dominates in the whole field region. The agreement between theory and measurement is regarded as an important step towards a more comprehensive understanding. The model predicts two distinct mechanisms and the condition for their dominance. These conditions result in an equivalence between field and defect density. The strong pinning behavior can be stabilized by means of a higher concentration at lower fields or vice versa. The coexistence of both mechanisms appears at fluences between about 10^{20} n/m^2 and 10^{21} n/m^2. This means that within one decade of defect concentration the transition between the weak and the strong pinning region is shifted from values close to the upper critical field to zero field.

The increase of F_p in the transition region between B_0 and B_p at a constant fluence can be as much as 2 orders of magnitude. Within that small-field region V_c shrinks in proportion to the square of F_p, neglecting the smooth field dependence of W. This extraordinary variation of V_c may be the reason for the observed large "history-effects" due to different unstable defect configurations of the FLL. We shall discuss this metastable phenomenon—which the collective theory does not account for—in a separate paper.

The correlation volume was calculated from F_p and W by the relation $V_c=W/F_p^2$. Table III shows the values at $b=0.5$, $B_{c2}=11.6$ T, and $\kappa=17.6$. V_c^{expt} was obtained by

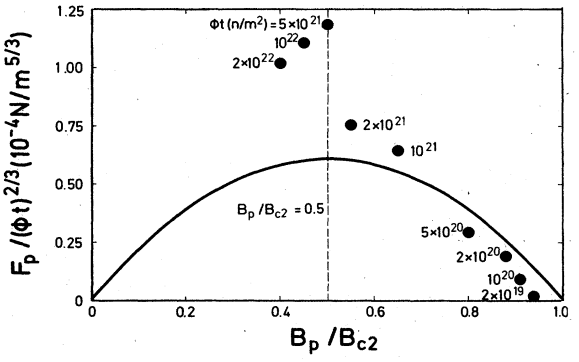

FIG. 11. Maximum pinning force density divided by the fast neutron fluence to the power of $\frac{2}{3}$ as a function of the corresponding reduced field B_p/B_{c2}. The experimental points are given by the solid circles whereas the solid line is calculated from Eq. (7) at $B_{c2}=11.6$ T, $\kappa=17.6$, and $q=2.6$. The dashed line indicates the expected minimum for B_p/B_{c2} of 0.5.

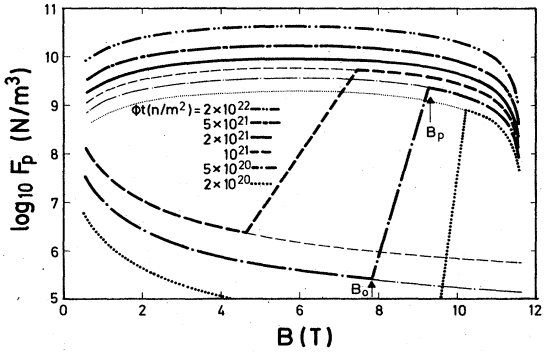

FIG. 12. Calculated volume pinning force F_p from Eqs. (2) and (6) as a function of magnetic field B for different fluences. The calculation is made for $B_{c2}=11.6$ T and $\kappa=17.6$.

the measured F_p values whereas V_c^{th} was calculated using Eq. (2) for $\phi t \leq 5\times10^{20}$ n/m^2 and Eq. (6) for $\phi t \geq 2\times10^{21}$ n/m^2, respectively. The difference between V_c^{expt} and V_c^{th} at $\phi t \leq 5\times10^{20}$ n/m^2 corresponds to the discrepancy of F_p between the experimental values and that calculated by Eq. (2), whereas the small difference in V_c at $\phi t \geq 2\times10^{21}$ n/m^2 results from the better agreement of F_p between the measurement and Eq. (6). Because the correlation volume in the low-F_p region is proportional to N^{-3}, it may be limited by the sample volume at the lowest fluences. In order to check whether the calculated correlation volume is meaningful, we made a speculative estimation of the radiation-induced defect concentration by means of the elementary threshold force f_{thr} in the nonlocal limit and the quantity W. Due to the weakly interacting defects, N should be larger than W/f_{thr}^2. For $B_{c2}=11.6$ T, $\kappa=17.6$, $B/B_{c2}=0.5$, we get $f_{\text{thr}}=4.4\times10^{-12}$ N and a lower limit of 1.3×10^{23} m^{-3} for the concentration at $\phi t=2\times10^{22}$ n/m^2. This results in a minimum number of about 60 defects within V_c. The number can be regarded as sufficient for using statistical arguments. At lower concentrations the condition for the minimum of V_c may change at least if R_c becomes of the order of the mean distance between pinning center defects. The estimated number of defects in V_c as well as the observed nonlinear field dependence and the metastable FLL configurations reject a single-particle pinning mechanism in the strong-pinning regime. In addition, a passing of the threshold criterion would not result in an equivalence between concentration and field, because the threshold force does not depend on the concentration.

V. CONCLUSIONS

The experimental investigation of the dependence of the volume pinning force on the concentration of weakly interacting defects reveals two distinct areas. At low concentration or at low fields a quadratic dependence $F_p \sim N^2$ dominates and results in very low pinning force densities. In the opposite area—at larger concentration or at higher fields—the exponent of the concentration dependence becomes increasingly smaller, together with pinning force densities larger by about two orders of magnitude. The field at which the transition between the two mechanisms takes place shifts with increasing concentration from the upper critical field to zero. Based on the collective theory of flux pinning, this equivalence of field and concentration at which the quadratic dependence vanishes corresponds to a transition into the nonlocal behavior of V_c. This changeover causes an enormous decrease of the correlation volume, i.e., a decrease in the number of defects which interact as a collective with the flux-line lattice, and results therefore in a more efficient interaction. The decrease of V_c is stopped if the transverse size of V_c becomes of the order of some flux-line lattice distances. Field and concentration of this maximum pinning force are consistent with the experimental values as well as those fields at which F_p starts to increase. The absolute values of F_p in dependence of the field agree only within one order of magnitude with the experimental ones. The main reason for this discrepancy may be the severe influence of different defect configurations of the FLL on the size of the correlation volume. In the strong-pinning case the experimental values of the pinning force density, as well as the theoretical ones, are far below the direct summation limit, i.e, a collective interaction governs both areas.

The impressive point of this comparison with the collective theory is the agreement with the prediction of the equivalence between field and concentration at which the strong pinning region dominates. This offers a convincing quantitative explanation of the "peak effect" observed at low defect concentration. It explains further the continuous change of the field dependence of F_p with increasing concentration up to a constant field dependence if the transition area is passed.

ACKNOWLEDGMENT

We gratefully thank A. M. Campbell for constructive and helpful discussions.

[1]E. H. Brandt, Phys. Lett. **77A**, 484 (1980).
[2]A. I. Larkin and Yu. N. Ovchinnikov, J. Low Temp. Phys. **34**, 409 (1979).
[3]H. R. Kerchner, J. Low Temp. Phys. **50**, 337 (1983).
[4]T. Matsushita and K. Yamafuji, J. Phys. Soc. Jpn. **50**, 38 (1981).
[5]R. Labusch, Cryst. Lattice Defects **1**, 1 (1969).
[6]A. M. Campbell, Philos. Mag. **37**, 149 (1978).
[7]P. H. Kes and C. C. Tsuei, Phys. Rev. Lett. **47**, 1930 (1981).
[8]E. H. Brandt, J. Low Temp. Phys. **53**, 41 (1983).
[9]H. R. Kerchner, D. K. Christen, C. E. Klabunde, S. T. Sekula, and R. R. Coltman, Jr., Phys. Rev. B **27**, 5467 (1983).
[10]A. M. Campbell and J. Evetts, Adv. Phys. **21**, 199 (1972).
[11]E. J. Kramer, J. Nucl. Mat. **72**, 5 (1978).
[12]T. Matsushita, J. Appl. Phys. **54**, 281 (1983).
[13]E. V. Thuneberg, J. Kurkijärvi, and D. Rainer, Phys. Rev. B **29**, 3913 (1984).
[14]H. Küpfer and A. A. Manuel, Phys. Status Solidi A **54**, 153 (1979).
[15]R. W. Rollins, H. Küpfer, and W. Gey, J. Appl. Phys. **45**, 5392 (1974).
[16]A. N. Polle and W. P. Voorbraak, ECN Report No. 83-117, 1983 (unpublished).
[17]R. Meier-Hirmer and H. Küpfer, J. Nucl. Mater. **108& 109**, 593 (1982).
[18]H. Küpfer, R. Meier-Hirmer and H. Scheurer, Physica **108B+C**, 1255 (1981).
[19]A. R. Sweedler, D. E. Cox, and S. Moehlecke, J. Nucl. Mater. **72**, 50 (1978).
[20]B. S. Brown, T. H. Blewitt, T. L. Scott, and D. G. Wozniak, J. Appl. Phys. **49**, 4144 (1978).
[21]M. Söll, K. Böhning, and H. Bauer, J. Low Temp. Phys. **24**, 631 (1976).
[22]E. H. Brandt, Phys. Status Solidi B **84**, 637 (1977).